# Mechanisms of carrier scattering in a compensated electron-hole plasma in deformed germanium at low temperatures

I. V. Kukushkin

*Institute of Solid State Physics, USSR Academy of Sciences*

(Submitted 3 June 1983)
Zh. Eksp. Teor. Fiz. **86**, 318–329 (January 1984)

Galvanomagnetic phenomena and the emission spectra of a photoexcited electron-hole (*e-h*) system were investigated in inhomogeneously deformed germanium. The times of electron scattering by acoustic phonons and excitons and of electron-hole scattering were determined for various temperatures ($T$) and densities ($n$) of the *e-h* system. It is shown that at $T = 2$–$8$ K and $n = (0.7$–$1.6)\times 10^{16}$ cm$^{-3}$, when Coulomb interaction of the electrons and holes predominates in the *e-h* system, the basic mechanism of carrier-momentum relaxation is *e-h* scattering.

## §1. INTRODUCTION

The transport properties of a photoexcited electron-hole (*e-h*) plasma in Ge have been investigated up to now only at sufficiently high temperatures ($T > 20$ K).[1,2] The reason is that in undeformed Ge at low temperatures ($T\sim 2$ K) it is impossible to control the plasma density in a wide range, since the *e-h* system breaks up into electron-hole liquid (EHL) drops of high density ($n = 2\times 10^{17}$ cm$^{-3}$) and a very rarefied gas of excitons and free carriers, $n \sim 10^{11}$ cm$^{-3}$ (Ref. 3), while the most interesting density range $n\sim 10^{13}$–$10^{16}$ cm$^{-3}$ lands in the two-phase region of the gas–EHL diagram and is inaccessible. The situation is substantially improved in the case of deformed Ge, when the destabilization of the EHL permits a dense gas of excitons and biexcitons to be obtained even at the very lowest temperatures.[4] When a critical density $n_c = 7\times 10^{15}$ cm$^{-3}$ is reached one can observe their ionizational destruction accompanied by an abrupt jump of the transport electronic properties.[5] Deformed Ge is therefore a convenient object for the study of scattering mechanism in photoexcited *e-h* systems with different densities.

Two fundamental types of carrier scattering can occur in semiconductors: scattering by the lattice (phonons, impurities, defects) and scattering of carriers by one another.[1)] In the former case the momentum acquired by the carrier in an external field becomes dissipated, whereas in the latter it remains inside the carrier system. This difference manifests itself, for example, in the fact that in an uncompensated *e-h* system the *e-e* and *e-h* scattering times ($\tau_{ee}$ and $\tau_{eh}$) can not determine the static conductivity even when these times are the very shortest. An exceptional system in this sense, in which $\tau_{eh}$ manifests itself, is an *e-h* system with equal numbers of electrons and holes.[6] This includes a system of photoexcited carriers in semiconductors (the scattering of carriers of one sign by one another cannot determine the static conductivity even in this case).

The mechanisms of the scattering of carriers in a photoexcited plasma at low temperatures were investigated so far on undeformed Ge and hence only at $n < 10^{11}$ cm$^{-3}$ (Refs. 7–10) and $n = 2\times 10^{17}$ cm$^{-3}$ (Refs. 11–14). One of the main methods of determining the relaxation times $\tau_p$ and $\tau_{eh}$ ($\tau_p$ is the time of momentum relaxation on acoustic phonons) in Ge at low temperatures at $n < 10^{11}$ cm$^{-3}$ is to study the cyclotron-resonance linewidths of photoexcited carriers.[7–10] This method was used to determine at $T = 1.8$ K in undeformed Ge the electron and hole scattering times $\tau_p^e$ and $\tau_p^h$, which were found to be $10^{-9}$ (Ref. 7) and $5\times 10^{-10}$ sec (Ref. 8), respectively. These values were obtained at a free-carrier density $n\sim 10^8$ cm$^{-3}$, when the *e-h* gas is classical, and in this case the known relation $\tau_p \sim T^{-3/2}$ is observed.[7] With increasing density of the *e-h* system, starting with $n > 10^{10}$ cm$^{-3}$, the cyclotron resonance linewidth increases linearly with $n$,[9] owing to the predominance of *e-h* scattering at $n > 10^{10}$ cm$^{-3}$. At $T = 1.8$ K and $n = 10^{11}$ cm$^{-3}$, the value of $\tau_{eh}$ is $2\times 10^{-10}$ (Ref. 9), and with further increase of the density the principal mechanism of the carrier momentum relaxation is electron-exciton scattering.[10] It is interesting that the temperature dependence of $\tau_{eh}$ at $n\sim 10^{11}$ cm$^{-3}$ is described by the known Brooks-Herring formula $\tau_{eh} \sim T^{3/2}$ (Ref. 9).

On the other hand, at $T\sim 2$ K and high excitation density, EHL drops are produced in undeformed Ge and comprise a compensated *e-h* plasma with equilibrium density $2\times 10^{17}$ cm$^{-3}$ (Ref. 3). In this case the times $\tau_p$ are usually determined from the mobility of the EHL drops in an inhomogeneous strain field.[11] The electron-hole collisions in these experiments do not lead to relaxation of the drop momentum as a whole, but they do establish the temperature of the carriers that move in the drop. The characteristic times $\tau_p$ at $T\sim 1.6$ K and $n = 2.3\times 10^{17}$ cm$^{-3}$ were found to be $10^{-8}$–$10^{-9}$ sec (Refs. 11 and 12).

Another method of determining the carrier momentum relaxation time in EHL drops is to study their transverse magnetoresistance $R_\perp(H)$. To this end one studies, as a function of the constant magnetic field, either the conductivity of thin Ge crystals completely filled with EHL,[13] or the absorption of the energy of an alternating magnetic field by the EHL drops.[14] As shown in Refs. 6 and 15, however, even in a compensated *e-h* plasma, where the resistivity at $H = 0$ can be determined by $\tau_{eh}$ ($\rho(0)\sim\tau_{eh}^{-1}$ at $\tau_{eh} \ll \tau_p$), the quantity $\tau_{eh}$ does not enter in the transverse magnetoresistance $\Delta\rho_\perp(H)$ (Refs. 6 and 15):

$$\Delta\rho_\perp(H)=\rho_\perp(H)-\rho_\perp(0)=\frac{H^2}{nc^2}\left(\frac{m_{ce}}{\tau_p^e}+\frac{m_{ch}}{\tau_p^h}\right)^{-1}. \quad (1)$$

 0038-5646/84/010183-07$04.00 © 1984 American Institute of Physics 

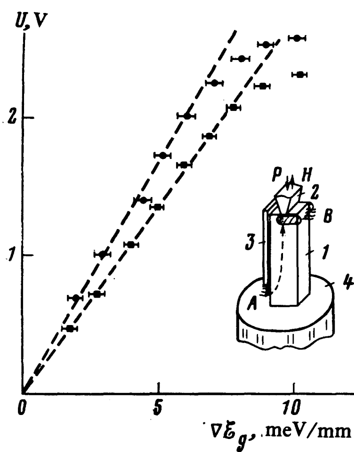


FIG. 1. Dependence of the no-load voltage $U$ in the PhVPM effect on the gradient of the band gap $\nabla \mathscr{E}_g$ in Ge⟨100⟩ (●) and Ge⟨111⟩ (■) at $H = 0.7$ T and $T = 2$ K. The inset shows the experimental setup: 1—sample, 2—brass prism, 3_black paper, 4—tin liner. $A$ and $B$ are two methods of exciting the crysal: $A$—to study the properties of the $e$-$h$ system in the potential well, $B$—to study the PhVPM effect. The region of the contacts soldered to the crystal is shaded.

Expression (1) can be represented in a form more convenient for the reduction of experimental data:

$$\rho_\perp(H) = \rho_\perp(0)\,(1+\omega_{ce}\omega_{ch}\tau_{eff}^2), \qquad (2)$$

Here $\omega_{ce}$ and $\omega_{ch}$ are the cyclotron frequencies of the electrons and holes, and $\tau_{\text{eff}}$ is the effective time, equal to $(\tau_p\tau_{eh})^{1/2}$ at $\tau_{eh} \ll \tau_p$ (see §4 for details). Thus, by measuring the transverse magnetoresistance it is possible to determine only a combination of $\tau_p$ and $\tau_{eh}$, so that to determine $\tau_{eh}$ it is necessary to measure independently $\tau_p$ and $\tau_{\text{eff}}$ for one and the same $e$-$h$ system. This possibility manifests itself in the study of the photovoltaic-piezomagnetic (PhVPM) effect in inhomogeneously compressed Ge.[5,16] The gist of this effect is that ionization destruction of the exciton produces a plasma filament that moves in the inhomogeneous-deformation field transversely to the magnetic field and, by virtue of the experimental geometry, wth ends joined to contacts (Fig. 1). The emf of such a photoelectric cell[17] depends only on $\tau_p$, and its internal resistance depends on $\tau_{\text{eff}} \approx (\tau_p\tau_{eh})^{1/2}$, so that $\tau_p$ and $\tau_{eh}$ can be determined independently.

## §2. EXPERIMENTAL TECHNIQUE

We investigated pure Ge single crystals measuring $3\times3\times10$ mm (as well as $2\times2\times10$ mm) with residual-impurity density $N \sim 10^{12}$ cm$^{-3}$ (the measurement results were independent of $N$ at $N \leqslant 3\times10^{14}$ cm$^{-3}$). Nonuniform uniaxial deformation was produced with a brass prism along a direction close to ⟨100⟩[2)] (deformation along ⟨111⟩ yields similar results, but the determination of $\tau_p$ and $\tau_{eh}$ is more complicated, see §3). A low pressure was applied at room temperature so that the knife edge of the prism became blunter (to a size $a \approx 0.7$ mm) and the crystal was pressed into a lower liner made of tin solder. After cooling to helium temperature, the pressure $P$ in the potential well could be varied to 800 MPa. The potential well produced in the interior of the crystal had in this case axial symmetry and its ends were joined to contacts.

Simultaneously with electric measurements we investigated the radiative-recombination spectra of the $e$-$h$ system, from which the system temperature and density as well as the pressure in the potential well and the gradient of the band gap[16,17] could be determined (the distance from the excited surface of the sample to the end point of the prism was chosen such that the Ge band gap could be measured directly from the surface of the crystal).

To measure the $e$-$h$ plasma density we recorded the spectra of the plasma emission with participation of $LA$ and $TA$ phonons (allowed and forbidden transitions, respectively), from whose integral intensity ratio the average density could be determined.[16,18]

The temperature of the $e$-$h$ system in the range 1.7–3 K was varied by pumping off $He^4$ vapor. To vary the crystal temperature in the 2–8 K range, the $He^4$ and the massive solenoid were cooled to 1.3 K and the $He^4$ vapor was set equal to 1 atm. Laser-radiation energy fed to the cryostat raised the temperature of the helium and of the solenoid monotonically to 4.2 K after more than an hour (at maximum incident power), after which intense boiling of the $He^4$ set in and the spectroscopic investigations became impossible. As the $He^4$ and solenoid temperature were raised to 4.2 K, the temperature of the $e$-$h$ system in the Ge at fixed pump differed substantially from that of the bath, rose from 3 to 10 K, and was determined from the ratio of the integral intensities of the $TA$ and $LA$ components of the emission spectra of the free exciton in the undeformed Ge (the load of the crystal was removed when the temperature of the $e$-$h$ system was determined). In undeformed germanium $I_{FE}^{TA}/I_{FE}^{LA} = 0.0025$ $T[K]$ (Ref. 18), and although the temperature of the crystal changed very slowly, it was determined by the described method before and after the electric measurements; the difference was included in the measurement error.

The nonequilibrium carriers were excited with an LT-2 cw laser ($\lambda = 1.064$ $\mu$m) of power up to 10 W. The spectral instrument was a double monochromator with 600 lines/mm gratings and with a dispersion 8 Å/mm in the operating range. The recombination radiation was registered with a cooled Ge(Cu) photoresistor in the synchronous detection regime at a modulation frequency 70 Hz. For the electric measurements, indium contacts were soldered to the lateral faces of the sample (see inset of Fig. 1). The contacts were always ohmic and were monitored against the change of the experimental data on reversal of the magnetic field direction.

## §3. SCATTERING OF FREE CARRIERS BY ACOUSTIC PHONONS

In pure Ge samples at low temperature, the principal mechanisms of the scattering of the photoexcited carriers in the $e$-$h$ system are the electron-phonon, electron-exciton, and electron-hole mechanism. Scattering by lattice defects and impurities was negligible in our case, since the measurement results were the same for different samples with different shallow-impurity densities (up to $N \sim 10^{14}$ cm$^{-3}$. The peculiarities of the electron-phonon scattering mechanism in semiconductors at low temperatures are, first, the fact

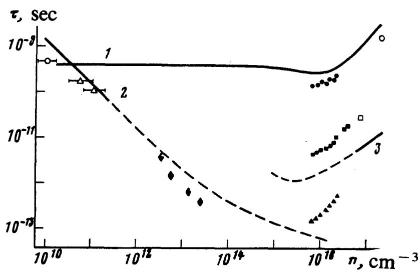


FIG. 2. Dependence of the free-carrier momentum relaxation time $\tau$ on their density in Ge⟨100⟩ at $T = 3$ K for different scattering mechanisms: $\tau_p$ (○,●); $\tau_{eh}$ (△,▲); $\tau_{\rm eff}$ (□,■); $\tau_{eex}$ (◆). Light symbols—data of Refs. 7–14, dark—results of present work. Curves, 1, 2, and 3 were obtained by calculating from Eqs. (3), (11), and (12), respectively.

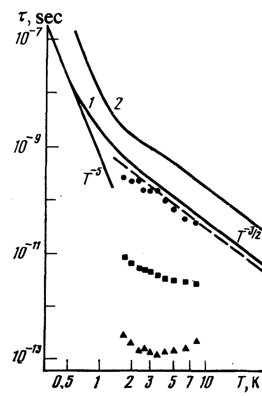


FIG. 3. Dependence of momentum relaxation time $\tau$ of free carriers on temperature in Ge⟨100⟩ at $n = 7\times10^{15}$ cm$^{-3}$ for different scattering mechanisms: $\tau_p$ (●); $\tau_{\rm eff}$ (■); $\tau_{eh}$ (▲). Curves 1 and 2—theoretical dependences of $\tau_p^e$ and $\tau_p^h$, calculated from Eq. (3) at $n = 7\times10^{15}$ cm$^{-3}$. The dashed line shows extrapolation of the $\tau_p^e(T)$ dependence obtained at $T \geqslant 20$ K (Ref. 1) in the temperature range $T = 2$–$10$ K.

that the thermal velocities of the carriers ($v_T$) at low e-h system densities are of the order of the speed of sound ($s$), and as a result at $2s > v_T > s$ the phonon emission is greatly hindered, and at $v_T < s$ it is utterly impossible.[19] Second, with increasing density of the e-h plasma quantum-statistical properties of the electrons and holes come into play and permit only the carriers on the Fermi surface to participate in the scattering processes. In the general case (but at $v_d \ll s$) the time of carrier scattering by acoustic phonons was obtained by Keldysh[20]:

$$\tau_p^{-1} = \frac{\pi}{3(2\pi)^4}\frac{mD^2}{\hbar^2 n\rho s}\left(\frac{kT}{\hbar s}\right)^5 \int_0^\infty x^4 \frac{e^x dx}{(e^x-1)^2} \times \ln\frac{e^x+\exp(-\alpha+{}^1/_4\beta)(x+\beta^{-1})^2)}{1+\exp(-\alpha+{}^1/_4\beta(x+\beta^{-1})^2)}, \quad (3)$$

where $\alpha = \mu/kT$; $\beta = kT/2ms^2$; $\mu$ is the chemical potential of a carrier system of density $n$ at a temperature $T$, $\rho$ is the density of the Ge crystal, $D$ is the deformation potential, $m$ is the state-density mass, and $v_d$ is the velocity of the plasma drift as a whole. The result of a computer calculation in accord with Eq. (3) is shown in Figs. 2 and 3 for the following values of the parameters: $m_e = 0.22\ m_0$; $m_h = 0.082\ m_0$; $D_e = 12$ eV; $D_h = 9$ eV; $\rho = 5.3$ g/cm$^3$; $s = 5\times10^5$ cm/sec (Refs. 1,3,21).

The times of carrier-momentum relaxation on acoustic phonons in a dense e-h plasma are determined in experiments from the drift of the EHL drops in an inhomogeneous deformation field.[11] In the PhVPM effect, the e-h plasma ($n = 7\times^{15}$ cm$^{-3}$) is produced as a result of ionization destruction of the excitons drifting in the inhomogeneous deformation field, when they reach critical density.[16] The no-load voltage ($U$) produced in the PhVPM effect because of the e-h plasma drift across the magnetic field ($H$) does not depend on $\tau_{eh}$ and is determined exclusively by the times $\tau_p^e$ and $\tau_p^h$ (Ref. 17):

$$U = \nabla\mathscr{E}_g LH(m_{ce}/\tau_p^e + m_{ch}/\tau_p^h)^{-1}, \quad (4)$$

where $\nabla\mathscr{E}_g$ is the gradient of the band gap, $L$ is the distance between the contacts, $m_{ce}$ and $m_{ch}$ are the carrier cyclotron masses. We used this circumstance for an experimental determination of the values of $\tau_p$. The only restriction on the applicability of (4) is the condition on the drift velocity: $v_d \ll s$. Since this condition is violated at sufficiently small $\Delta\mathscr{E}_g \times 10$ meV/mm,[22] we have determined experimentally the $\Delta\mathscr{E}_g$ region in which (4) is well satisfied. Figure 1 shows $U(\nabla\mathscr{E}_g)$ plots for Ge⟨100⟩ and Ge⟨111⟩ at $H = 0.7$ $T$ and $T = 2$ K, from which it is seen that the condition for the applicability of (4) is $\nabla\mathscr{E}_g < 7$ meV/mm, corresponding to uniaxial strains $P < 60$ MPa for Ge⟨111⟩ and $P < 300$ MPa for Ge ⟨100⟩. In Ge⟨111⟩ at $P < 60$ MPa the structure of the valence band is very complicated.[23] We therefore investigated in the present study the PhVPM effect in Ge⟨100⟩, where at $P = 300$ MPa the splitting of the valence band is 10 meV and it can be regarded with good accuracy as parabolic with masses $m_h^\parallel = 0.0457\ m_0$, $m_h^\perp = 0.1094\ m_0$. In Ge⟨100⟩ we have $m_{ce}/\tau_p^e \approx 8\ m_{ch}/\tau_p^h$ (Fig. 2) and, as can be seen from (4), the no-load voltage is determined mainly by the electron scattering time $\tau_p^e$.

Figure 4 shows plots of $U(H)$ in Ge⟨100⟩ at $\nabla\mathscr{E}_g = 6$ meV/mm and at different excitation densities[3)] (Fig. 4a) and temperatures (Fig. 4b), from which we determined the times $\tau_p^e$. We note that in the present study all the measurements were made in magnetic fields $H < 1$ T in order to exclude

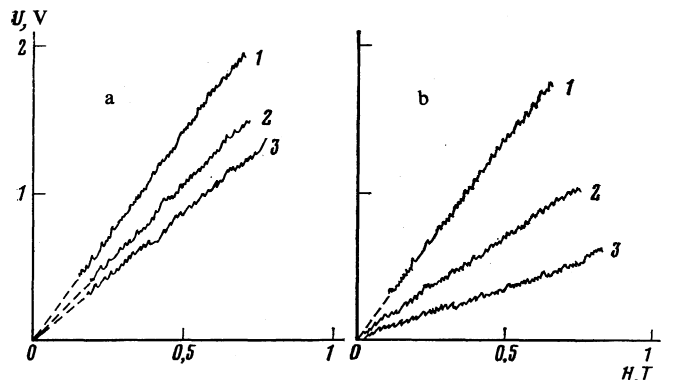


FIG. 4. Dependence of the no-load voltage $U$ on the magnetic field $H$ in Ge⟨100⟩ at $\Delta\mathscr{E}_g = 4$ meV/mm at different excitation powers (a) and temperatures (b): a) $T = 3$ K; $W_1 = 0.5$ W ($n_1 = 7\times10^{15}$ cm$^{-3}$), $W_2 = 1.5$ W ($n_2 = 9\times10^{15}$ cm$^{-3}$), $W_3 = 2.6$ W ($n_3 = 1.7\times10^{15}$ cm$^{-3}$); b) $W = 0.7$ W ($n = (7\pm1)\times10^{15}$ cm$^{-3}$); $T_1 = 1.9$ K; $T_2 = 3.8$ K; $T_3 = 5.2$ K.

quantum effects that influence substantially the kinetic phenomena in semiconductors in stronger fields.[24] A change of the excitation power from 0.5 to 2.5 W permitted variation of the average *e-h* plasma density in the range $(0.7–1.7)\times 10^{16}$ $cm^{-3}$, which was determined from the ratio of the integral intensities of the *TA* and *LA* components of its emission spectrum.[16] We note that although the density of the *e-h* pairs in the plasma filament is most likely not constant, the quantity determined from the ratio of the integral intensities of the plasma emission lines is an average in the sense that it corresponds to the density of the main fraction of the carriers. From Fig. 2, in which the circles show the experimental $\tau_p^e(n)$ dependence and the solid line the theoretical calculated from Eq. (3), it can be seen that the experimental and theoretical dependences are close and behave similarly in the density range $(0.7–1.7)\times 10^{16}$ $cm^{-3}$. The growth of $\tau_p^e$ with $n$ is due to quantum statistical properties of the electron gas.

The temperature dependence of $\tau_p^e$ at $\nabla\mathscr{E}_g = 6$ meV/mm and $W = 0.7$ W is shown by circles in Fig. 3. At $W = 0.7$ W and with the temperature varied from 2 to 8 K the *e-h* plasma density remained practically constant, $(7 \pm 1)\times 10^{15}$ $cm^{-3}$, and the parameter $\mu_e/kT$ changed from 2 to $-1$, so that the electron gas exhibits the $\tau_p^e \sim T^{-3/2}$ dependence typical of the nondegenerate case. For comparison, the solid lines 1 and 2 in the same figure show the theoretical plots of $\tau_p^e(T)$ and $\tau_p^h(T)$, calculated from Eq. (3) at a fixed density $n = 7\times 10^{15}$ $cm^{-3}$, while the dashed line shows the $\tau_p^e(T)$ plot obtained by extrapolating into the $T = 2–8$ K temperature region the values of obtained experimentally at $T > 30$ K for a classical electron gas.[1] It can be seen that the agreement is quite satisfactory.

The study of the no-load voltage in the PhVPM effect has thus permitted a determination of $\tau_p^e$ in a dense compensated *e-h* plasma; determination of $\tau_{eh}$ in this plasma calls for measurements of the transverse magnetoresistance.

## §4. ELECTRON-HOLE SCATTERING

A dense compensated *e-h* plasma is unique in the sense that its static conductivity is determined by the *e-h* scattering time if $\tau_{eh} \ll \tau_p$ (Ref. 6):

$$\sigma = ne^2\tau_{eh}(m_e+m_h)/m_e m_h$$

However, as shown in Refs. 6 and 15, there is no transverse magnetoresistance due to scattering between carriers: $\Delta\rho_\perp(H)$ cannot depend on $\tau_{eh}$ (and $\tau_{ee}$). The reason is that the conductivity in a transverse magnetic field reduces to motion of the centers of the electron and hole orbits along and counter to the direction of the electric field. In *e-h* collisions the centers of orbits of the scattered particles shift to one side, and consequently such processes cannot contribute to the conductivity. The change of the conductivity of a dense compensated *e-h* plasma in a transverse magnetic field is completely determined by the carrier scattering by the lattice (phonons, impurities, defects). Following Refs. 6 and 15 we can express $\rho_\perp(H)$ in the form (2), where

$$\tau_{eff}^2 = \tau_p^e\tau_p^h\tau_{eh} \bigg/ \left(\tau_{eh} + \frac{m_{ce}\tau_p^h + m_{ch}\tau_p^e}{m_{ce}+m_{ch}}\right). \qquad (5)$$

The quantity $\tau_{\rm eff}^2$ usually determined in experiment contains $\tau_{eh}$, and at $\tau_{eh} \ll \tau_p$ we have $\tau_{\rm eff}^2 \approx \tau_p\tau_{eh}$, where $\tau_p$ is the shorter of the times $\tau_p^e$ and $\tau_p^h$.

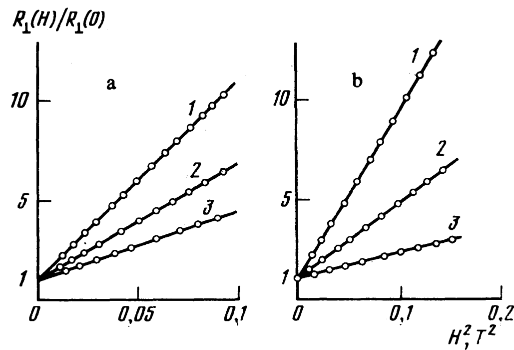


FIG. 5. Dependence of transverse magnetoresistance $R_\perp(H)$ on $H^2$ in Ge⟨100⟩ at various excitation powers (a) and temperatures (b): a) $T = 3$ K; $W_1 = 2.4$ W ($n_1 = 1.6\times 10^{15}$ $cm^{-3}$), $W_2 = 1.8$ W ($n_2 = 10^{16}$ $cm^{-3}$), $W_3 = 0.6$ W ($n_3 = 7\times 10^{15}$ $cm^{-3}$); b) $W = 0.7$ W ($n = 7\times 10^{15}$ $cm^{-3}$), $T_1 = 2$ K, $T_2 = 3.5$ K, $T_3 = 8$ K.

A photocell based on the PhVPM effect has a strictly ohmic current-voltage characteristic in the excitation density range $0.5\ W < W < 2.5$ W (Ref. 17), and has therefore a definite internal resistance $R = U/J$, where $J$ is the short-circuit current of the photocell. The radiation intensity of the plasma filament and the average density of the carriers in it do not depend on $H$ up to $H = 2$ T (Ref. 16), so that its volume and cross section ($L$ = const) do not change in these fields. The change of the internal resistance of the photocell in a transverse magnetic field is therefore due only to a change of the specific conductivity and is determined entirely by the transverse magnetoresistance.

Figures 5a and 5b show plots of $R_\perp(H^2)$ for different temperatures and densities of the *e-h* plasma; in accord with (2) and (5), these plots are straight lines. The values of $\tau_{\rm eff}$ obtained from $R_\perp(H^2)$ at different $T$ and $n$ are shown by the squares in Figs. 2 and 3 and are in fair agreement with the data of Refs. 13 and 14. Having independent measurements of $\tau_p^e$ (which are substantially shorter than $\tau_p^h$) and of $\tau_{\rm eff}$, we can determine from (5) the value of $\tau_{eh}$. The $\tau_{eh}(n)$ and $\tau_{eh}(T)$ dependences are shown by the triangles in Figs. 2 and 3 respectively. The distinguishing feature of *e-h* scattering is the increase of $\tau_{eh}$ with increasing temperature, observed at $T > 3$ K (see Fig. 3), when an electron gas with $n\times 7\times 10^{15}$ $cm^{-3}$ is found to be nondegenerate. The reason is that in a nondegenerate gas a temperature rise increases the average kinetic energy of the electrons, and hence decreases the cross section for their scattering by the holes. At $T < 3$K the decisive factor is $\mathscr{E}_{Fe}\mathscr{E}_{Fh}/(kT)^2$, which is of quantum-statistical origin[25] (here $\mathscr{E}_{Fe}$ and $\mathscr{E}_{Fh}$ are the Fermi energies of the electrons and holes). For the same reason, an increase of $\tau_{eh}$ with increasing $n$ is observed in Fig. 2 at $T = 3$ K.

The functions $\tau_{eh}(n)$ and $\tau_{eh}(T)$ have thus minima $\tau_{eh}^{\rm min}$ at $n_0$ and $T_0$, when the chemical potential of the electron gas vanishes and a noticeable role is assumed by the quantum statistical factor $\mathscr{E}_{Fe}\mathscr{E}_{Fh}/(kT)^2$, i.e., on satisfaction of the condition

$$n_0 = \frac{1}{\pi^2}\left(\frac{2m_e kT}{\hbar^2}\right)^{3/2} F_{1/2}(0).$$

Although the accessible range of densities and pressures was small in this study, nonetheless the value of $\tau_{eh}^{min}$ was practically independent in it of $n$ and $T$, and amounted to $(1-1.5)\times 10^{-13}$ sec. We note, first, that the characteristic "Coulomb" time $\tau = \hbar/\mathrm{Ry} = 2.4\cdot 10^{-13}$ sec is close to the value of $\tau_{eh}^{min}$ and, second, that a similar $\tau_{eh}(n)$ dependence with $\tau_{eh}^{min} \approx 10^{-13}$ sec was observed at high temperatures ($T = 20$–$300$ K) in Ref. 2.

## §5. ELECTRON-EXCITON SCATTERING

So far we have investigated the electron transport properties of the system at excitation densities higher than the Mott value ($n_e = 7\times 10^{15}$ cm$^{-3}$ in Ge, Ref. 16), when practically all the excitons are ionized because of the screening of the Coulomb interaction. On the other hand, at $n < n_e$ the dominant role in the $e$-$h$ system is assumed by excitons and biexcitons, whose density in Ge⟨100⟩ at $T \approx 2$ K can reach $1.5\times 10^{15}$ cm$^{-3}$ and $2\times 10^{15}$ cm$^{-3}$, respectively.[4] In such a system the conductivity can be determined by electron-exciton and electron-biexciton collisions, using the notation $e$-$ex$ and $\tau_{eex}$). It is interesting that although formally the $e$-$ex$ scattering mechanism cannot be regarded as being of the lattice type (in the classification of Ref. 6), in transverse magnetoresistance it is completely analogous to the lattice mechanisms, since scattering of an electron by an electrically neutral exciton is accompanied by charge transfer, so that this scattering mechanism can determine the static conductivity in a transverse magnetic field.

The $e$-$ex$ scattering mechanism was studied in undeformed Ge at $T = 4.2$ K and at an $e$-$h$ system density $\sim 10^{13}$ cm$^{-3}$ in Ref. 10, where it was shown that it is similar to electron scattering by a neutral impurity, for whch[26]:

$$\tau^{-1}=\frac{5N\hbar e^2}{2\pi\varkappa E_i\mu_x}=\frac{20\hbar^3\varkappa N}{e^2\mu_x^{\,2}}, \tag{6}$$

where $N$ is the density of the neutral impurities (excitons), $\varkappa$ is the dielectric constant of Ge, $E_i$ is the impurity (exciton) ionization energy, and $\mu_x$ is the reduced mass of the electron and impurity (exciton). Inasmuch as at neutral-impurity densities $10^{14}$–$10^{15}$ cm$^{-3}$ the electron-impurity scattering mechanism predominates at low temperatures[27] ($T \approx 2$ K), the $e$-$ex$ mechanism is expected to determine the static conductivity of the system at $T \approx 2$ K and at a density $\sim 10^{15}$ cm$^{-3}$ both in the absence and in the presence of a transverse magnetic field:

$$R_\perp(H)=R_\perp(0)\,(1+\omega_{ce}\omega_{ch}\tau_{eex}^2), \tag{7}$$

$$R_\perp(0)=\frac{L}{S}\frac{m}{ne^2\tau_{eex}}, \tag{8}$$

where $L$ is the distance between the contacts and $S$ is the cross section.

In the present work we studied the transverse magnetoresistance of an $e$-$h$ system in an axisymmetric potential well with terminal contacts (**H**‖**P**‖⟨100⟩, see Fig. 1). To exclude breakdown and drift of the $e$-$h$ plasma in the crossed electric and magnetic field it was necessary to use an electric field $E < 10^{-2}$ V/cm (Ref. 13). Therefore to exclude the photo-voltaic-magnetic fields of scale $\sim 1$ V/cm (Ref. 16) the experimental conditions were made such that the photoexcited carriers drifted in the potential well practically in the magnetic field direction.

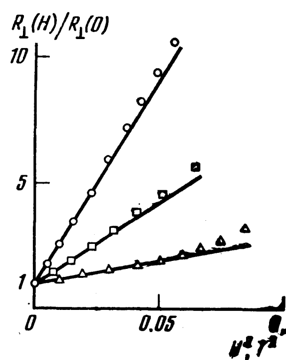


FIG. 6. Dependence of transverse magnetoresistance $R_\perp(H)$ in $e$-$h$ system in Ge⟨100⟩ on $H^2$ at $T = 2.2$ K, $P = 480$ MPa, and different excitation powers: $W = 20$ mW, $n_g = 1.2\times 10^{14}$ cm$^{-3}$ (○); $W = 35$ mW, $n_g = 1.8\times 10^{14}$ cm$^{-3}$ (□); $W = 90$ mW, $n_g = 4\times 10^{14}$ cm$^{-3}$ (△).

In Fig. 6 are shown typical $R_\perp(H^2)$ plots at different values of the exciton and biexciton gas density ($n_g$) determined from the radiative-recombination spectra. (The deviation of the $R_\perp(H^2)$ plots from straight lines, due to change of the exciton ionization energy in the magnetic field,[28] was significant only at $H > 0.5$ T.) The pesence of two emission lines, of excitons ($FE$) and of biexcitons ($M$), makes it possible to determine with good accuracy, from the ratio of the integral intensities of these lines ($I_M/I_{FE}$), the chemical potential $\mu_{ex}$ of the gas phase, and the densities of the excitons ($n_{ex}$) and biexcitons ($n_M$) (Ref. 4):

$$I_M/I_{FE}=2.3\cdot\sqrt{2}\exp\left(-\frac{|\mu_{ex}|-\Delta_M}{kT}\right), \tag{9}$$

$$n_i=g_i\frac{(m_ikT)^{3/2}}{\sqrt{2}\,\pi^2\hbar^3}\int_0^\infty\frac{z^{1/2}dz}{\exp(z-\mu_i/kT)-1},\quad i=ex, M, \tag{10}$$

where $g_{ex} = 4$, $g_M = 1$; $\mu_M = 2\mu_{ex} + \Delta_M$; $\Delta_M = 0.27$ meV (Ref. 28) is the biexciton binding energy. The value of $\tau_{eex}$ determined from $R_\perp(H^2)$ turned out to be sensitive to only one parameter, the exciton and biexciton gas density $n_g$, and was independent, *e.g.*, of the temperature at constant $n_g$.

Figure 7 shows the $\tau_{eex}(n_g)$ dependence at $T = 2.2$ K; it

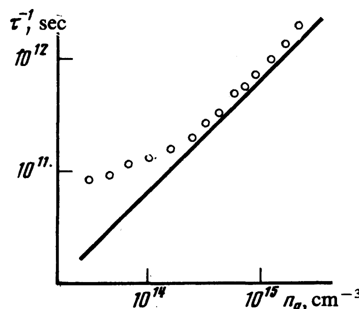


FIG. 7. Dependence of momentum relaxation time $\tau$ on the exciton and biexciton as density $n_g$ in Ge⟨100⟩ at $P = 480$ MPa and $T = 2.2$ K. The straight line shows the $\tau_{eex}(n_g)$ dependence calculated from Eq. (6).

agrees well, in the density range $2\times10^{14}$–$2\times10^{15}$ cm$^{-3}$, with the theoretical dependence calculated from Eq. (6). The deviation from a straight line at $n_g < 2\times10^{14}$ cm$^{-3}$ corresponds to a change of the dominant scattering mechanism, and judging from the temperature dependence ($\tau_{\rm eff}$ increases like $\sim T^{+0.4}$) with rising temperature at $n_g < 2\times10^{14}$ cm$^{-3}$, the shortest momentum relaxation time corresponds in this case to the *e-h* scattering mechanism.

Besides measurements of the transverse magnetoresistance at $n_g < 7\times10^{15}$ cm$^{-3}$, we have also investigated $R_\perp(H)$ in an EHL with $n = (1.4$–$3)\times10^{16}$ cm$^{-3}$, which filled completely the axisymmetric potential well. These measurements agreed well with the results of §4 and permitted a determination of the cross-section area of the potential well: $S = 0.7\pm0.1$ mm$^2$ (this value was practically independent of the *e-h* plasma density and temperature). The obtained value of $S$, as well as the exciton emission *FE* line shape, confirms the conclusions[22] that at large strains and close dimensions of the crystal ($L = 2$ mm) and of the knife edge of the deforming prism ($a\approx0.7$ mm) the result $S\sim a^2$ depends little on the carrier energy.

An independent measurement of $\tau_{eex}$ using transverse magnetoresistance yielded the free-carrier density $n$, which did not exceed $3\times10^{13}$ cm$^{-3}$ at $T = 3$ K all the way to the condensation of the excitons in the EHL drop. A plot of $\tau_{eex}(n)$ at $T = 3$ K is shown in Fig. 2.

## §6. DISCUSSION OF RESULTS

The mechanisms of carrier scattering in a photoexcited plasma at low temperatures were investigated experimentally in Refs. 7–14 in the region of low densities $n < 10^{12}$ cm$^{-3}$ and very high ones $n > 0.7\times10^{17}$ cm$^{-3}$. A summary of the available experimental and theoretical data is presented in Fig. 2. In the present work we studied the density range $(0.7$–$1.7)\times10^{16}$ cm$^{-3}$, which is of interest primarily because *e-h* scattering in this system turns out to be strongest, since the carrier density is already high enough and the quantum-statistical factor $\mathscr{E}_{Fe}\mathscr{E}_{Fh}/(kT)^2$ is still close to unity, so that practically all the particles can participate in the scattering processes. In addition, at $T\sim2$–$7$ K it is just the Coulomb interaction between the electrons and the holes which predominates in this system (the characteristic energy of this interaction is ${\rm Ry} = e^4\mu_0/2\varkappa^2\hbar^2 = 2.65$ meV, whereas the average kinetic energy of the carriers is $\langle\mathscr{E}\rangle \langle 1$ meV at $n = 7\times10^{15}$ cm$^{-3}$). We note that there is no theory of *e-h* scattering with dominant Coulomb interaction, although two approaches are usually discussed in the literature. The first[9] is based on the known Brooks-Herring formula obtained for scattering by a screened Coulomb center (ionized impurity):

$$\tau_{eh}^{-1}=8\pi nv\,(e^2/4\varkappa\langle\mathscr{E}\rangle)^2(\ln(1+\Delta^{-1})+(1+\Delta)^{-1}), \qquad (11)$$

where $\Delta = \hbar^2/4\mu_0^2v^2a_0^2$, $\varkappa$ is the dielectric constant, $a_0$ is the screening radius, $\mu_0$ is the reduced mass of the electron and hole, and $v$ is the average carrier velocity. Equation (11) was obtained by Brooks and Herring[29] in the Born approximation for a nondegenerate electron gas of low density, and the condition for its applicability is ${\rm Ry}\ll\langle\mathscr{E}\rangle = 1.5\,kT$. An expression similar to (11) for $\tau_{eh}$ can be found in the theory of classical plasma,[30] in which the small parameter is the ratio of the average Coulomb energy to the temperature $g = e^2n^{1/3}/\varkappa kT\approx{\rm Ry}/r_s kT\ll1$. In this case the correlation effects are negligibly small ($\sim g$) and it is therefore not surprising that expression (11) describes correctly the experimental data obtained in Ref. 9 at $n < 10^{11}$ cm$^{-3}$ and $T = 3$ K. On the other hand, in the plasma studied in the present paper ($n = 7\times10^{15}$ cm$^{-3}$, $T\sim3$ K), the Coulomb interaction of the carriers predominates and the parameter $g > 2$. Nonetheless, as seen from Fig. 2, the values of $\tau_{eh}$ obtained at $T = 3$ K in §4 are also described fairly well by Eq. (11) (curves 3 of Fig. 2), and the agreement is particularly good if account is taken in expression (11) of the quantum-statistical factor $\langle\mathscr{E}_e\rangle\langle\mathscr{E}_h\rangle/(1.5\,kT)^2$. In addition, if we substitute in (11) the density at which the transition from a classical plasma to a degenerate with $n\approx(mkT/\hbar^2)^{3/2}$ is realized and the weak logarithmic function is neglected, then $\tau_{eh}^{\rm min} = \hbar/{\rm Ry}$, in agreement with the experiment.

Another expression for $\tau_{eh}$ was proposed in Ref. 31:

$$\tau_{eh}^{-1}=(4\pi n/3)^{1/3}(v_{Fe}v_{Fh})^{1/2}(kT)^2/\mathscr{E}_{Fe}\mathscr{E}_{Fh}, \qquad (12)$$

wehre $v_{Fe}$ and $v_{Fh}$ are the Fermi velocities of the carriers, and $\mathscr{E}_{Fe}$ and $\mathscr{E}_{Fh}$ are their Fermi energies. It is easily seen that Eq. (12) accounts for only the quantum statistics of the carriers and for the average interparticle path time, but the Coulomb interaction of the electrons and holes is completely absent. It is therefore to be expected that expression (12) will describe $\tau_{eh}$ correctly only at $r_S\ll1$, when the Fermi energies of the carriers are substantially larger than their Coulomb-interaction energies (in particular, Eq. (12) may turn out to be valid for semimetals). The values of $\tau_{eh}$ calculated from (12) (curve 3 of Fig. 2) are somewhat higher than the experimental), obviously because of the neglect of the Coulomb scattering cross section in (12). On the other hand, from Eq. (12) we can determine $\tau_{eh}$ of uncorrelated electrons and holes (i.e., without allowance for Coulomb effects) and to determine the gain $g_{eh}(0)$ which is equal, by definition, to the ratio of the probabilities of finding the electron at the hole location in the case of correlated and uncorrelated carriers.[3] If this approach were legitimate it would permit, at different $n$ and $T$, a determination of the value of $g_{eh}(0)$, which is of particular interest to the theory, for it is precisely this parameter which is most sensitive to the theoretical approximations.[32] The value of $g_{eh}(0)$ at $T = 2$ K and $n = 7\times10^{15}$ cm$^{-3}$ ($r_s\approx2$), obtained by such a procedure, is $10\pm1$ and is close to the values obtained in Ref. 33.

It is interesting that the momentum transport relaxation time obtained from galvanomagnetic investigations in the case of electron-hole scattering does not conform to the energy uncertainty $\Delta\mathscr{E} = \hbar/\tau_{eh}\approx4$ meV that would manifest itself as a broadening of the radiative-recombination spectra of an *e-h* plasma, since the halfwidth of the emission line of the plasma $P$ is $\sim2$ meV (Refs. 4,16) and, for example, is practically independent of temperature, whereas $\tau_{eh}$ depends on it substantially (Fig. 3). The apparent reason is that in recombination of electrons and holes (which is well described in the single-particle approximation even at $n = 7\times10^{15}$ cm$^{-3}$ and $T = 3\,K$, Ref. 34), the *e-h* scattering, being an internal process, can determine $\Delta\mathscr{E}$ of each of the

particles, but does not influence the combined energy of recombining carriers, which is the one that manifests itself in the emission spectrum. An answer to this question, however, requires a rigorous solution and can be of definite interest from the theoretical standpoint.

Thus, in a compensated *e-h* plasma in deformed Ge, at low temperatures and at densities $n \sim 7 \times 10^{15}$ cm$^{-3}$ ($r_s \approx 2$), when Coulomb interaction predominates in the carrier system, the principal momentum relaxation mechanism is electron-hole scattering. The *e-h* scattering time depends strongly on density and temperature, and the minimum value of $\tau_{eh}$ is reached on going from a classical *e-h* plasma to a degenerate one, and amounts to $\sim \hbar$/Ry.

In conclusion, the author is deeply grateful to V. F. Gantmakher, S. É. Esipov, S. V. Iordanskii, V. D. Kulakovskii, I. B. Levinson, Ya. E. Pokrovskiĭ, and V. B. Timofeev for exceedingly helpful discussions.

[1)]Carrier scattering by excitons, which predominates at low temperatures and at *e-h* gas densities $\sim 10^{15}$ cm$^{-3}$, turns out to be similar to electron-impurity scattering and is therefore included in the first type (see §5).

[2)]The deflection from ⟨100⟩ was $\sim 5°$ and was necessary to lift degeneracies in the conduction band.

[3)]To maintain constant crystal temperature the bath temperature was varied when the excitation power was varied.


[1]E. M. Conwell, High-Field Transport in Semiconductors. Suppl. 9 to Solid State Phys., Academic, 1967.
[2]J. R. Meyer and M. Glicksman, Phys. Rev. **B17**, 3227 (1978).
[3]J. C. Hensel, T. G. Phillips, and G. A. Thomas, Sol. St. Phys. **32**, 87 (1977).
[4]I. V. Kukushkin and V. D. Kulakovskiĭ, Zh. Eksp. Teor. Fiz. **82**, 900 (1982) [Sov. Phys. JETP **55**, 528 (1982)].
[5]I. V.Kukushkin, V. D. Kulakovskiĭ, and V. B. Timofeev, Pis'ma Zh. Eksp. Teor. Fiz. **35**, 367 (1982) [JETP Lett. **35**, 451 (1982)].
[6]V. F. Gantmakher and I. B. Levinson, Zh. Eksp. Teor. Fiz. **74**, 261 (1978) [Sov. Phys. JETP. **47**, 133 (1978)].
[7]R. Ito, H. Manamura, and H. Fukai, Phys. Lett. **13**, 26 (1964).
[8]J. C. Hensel and K. Suzuki, Phys. Rev. **B9**, 4219 (1974).
[9]H. Kawamura, H. Saji, M. Fukai, K. Sekido, and I. Imai, J. Phys. Soc. Jpn. **19**, 288 (1964).
[10]T. Ohyama, T. Sanada, T. Yoshihara, K. Murase, and E. Otsuka, Phys. Rev. Lett. **27**, 33 (1971).
[11]A. S. Alekseev, V. S. Bagaev, and T. I. Galkina, Zh. Eksp. Teor. Fis. **63**, 1020 (1972) [Sov. Phys. JETP **36**, 536 (1973)].
[12]A. S.Alekseev, T. I. Galkina, V. N. Maslennikov, R. G. Khakimov, and E. P. Shchebnev, Pis'ma Zh. Eksp. Teor. Fiz. **21**, 578 (1975) [JETP Lett. **21**, 271 (1975)].
[13]V. M. Asnin and N. I. Mirtskhulava, Fiz. Tverd. Tela (Leningrad) **21**, 3677 (1979) [Sov. Phys. Solid State **21**, 341 (1979)].
[14]Bogdanov and Ya. E. Pokrovskiĭ, Zh. Eksp. Teor. Fiz. **83**, 2329 (1982) [Sov. Phys. JETP **56**, 1350 (1983)].
[15]S. A. Kukkonen and P. F. Maldague, Phys. Rev. **B19**, 2394 (1979).
[16]I. V. Kukushkin, V. D. Kulakovskiĭ, T. G. Tratas, and V. B. Timofeev, Zh. Eksp. Teor. Fiz. **84**, 1145 (1983) [Sov. Phys. JETP **57**, 665 (1983)].
[17]S. É. Esipov and I. V. Kukushkin, Fiz. Tverd, Tela (Leningrad) **26**, 382 (1984) [Sov. Phys. Solid State **26**, 227 (1984)].
[18]C. Benoit a la Guillaume, M. Voos, and F. Salvan, Phys. Rev. **B5**, 3079 (1972).
[19]P. A. Kalauskas and I. B. Levinson, Litov. fiz. sbornik **6**, 33 (1966).
[20]L. V. Keldysh, Éksitony v poluprovodnikakh (Excitons in Semiconductors), Nauka, 1971, p. 5.
[21]F. Blatt, Solid State Phys. **4**, 1999 (1957).
[22]I. V. Kukushkin and V. D. Kulakovskiĭ, Fiz. Tverd. Tela (Leningrad) **25**, 2360 (1983) [Sov. Phys. Solid State **25**, 1355 (1983)].
[23]G. Kirczenow and K. S.Singwi, Phys. Rev. **B19**, 2117 (1979).
[24]Sh. M. Kogan, V. D. Shcadrin, and A. Ya. Shul'man, Zh. Eksp. Teor. Fiz. **68**, 1377 (1975) [Sov. Phys. JETP. **41**, 686 (1975)].
[25]C. Kittel, Quantum Theory of Solids, Wiley, 1963.
[26]C. Erginsoy, Phys. Rev. **79**, 1013 (1950).
[27]A. E. Zhidkov and Ya. E. Pokrovskiĭ, Zh. Eksp. Teor. Fiz. **78**, 1589 (1980) [Sov, Phys. JETP **51**, 798 (1980)].
[28]V. L. Kulakovskiĭ, I. V. Kukushkin, and V. B. Timofeev, *ibid.* **81**, 684 (1981) [**54**, 366 (1981)].
[29]H. Brooks, Phys. Rev. **83**, 879 (1951) [*sic*!].
[30]A. I. Akhiezer, I. A. Akhiezer, R. V. Polovin, A. G. Sitenko, and K. N Stepanov, Élektrodinamika plazmy (Plasma Electrodynamics), Nauka, 1974.
[31]A. Monoliu and C. Kittel, Sol. St. Commun. **21**, 635 (1977).
[32]T. M. Rice, Sol. St. Phys. **32**, 1 (1977).
[33]P. Vashita, P. Bhattacharyya, and K. S. Singwi, Phys. Ref. Lett. **30**, 1248 (1973).
[34]I. V. Kukushkin, Zh. Eksp. Teor. Fiz. **84**, 1840 (1983) [Sov. Physe. JETP **57**, 1072 (1983)].


Translated by J. G. Adashko